Shallow pellet fuelling under conditions of RMP ELM mitigation or divertor detachment in ASDEX Upgrade

M Valovič[1], M Bernert[2], P T Lang[2], A Kirk[1], W Suttrop[2], D Brida[2], M Cavedon[2], M Dunne[2], R Fischer[2], L Garzotti[1], L Guimarais[2], F Janky[2], N Leuthold[2], PJ Mc Carthy[3], A Mlynek[2], B Ploeckl[2], E Poli[2], G Tardini[2], E Viezzer[2], E Wolfrum[2], the ASDEX Upgrade team[2] and the EUROfusion MST1 team[4]

[1]*CCFE, Culham Science Centre, Abingdon, OX14 3DB, UK;*
[2]*Max-Planck-Institut für Plasmaphysik, Boltzmannstrasse 2, D-85748 Garching, Germany;*
[3]*Department of Physics, University College Cork, Cork, Ireland;*
[4]*See H. Meyer et al., Nucl. Fusion 57 (2017) 102014*

Introduction

In ITER, injection of hydrogen isotope pellets will be the main plasma density control tool. The pellets will be injected from the high field side to maximise the deposition depth, which will be still relatively shallow. This plasma periphery is subject to ELM control and divertor detachment control and therefore the interaction of pellet fuelling with these loops might be expected. This paper presents the results of such experiments in ASDEX Upgrade where pellets are used [1] to control plasma density under conditions of ELM control or divertor detachment. In these experiments direct fuelling by gas is negligible to mimic the ITER fuelling condition in the plasma core. The relative pellet size and pellet deposition are aimed to approach those in ITER. ELMs are controlled by n=2 Resonant Magnetic Perturbations (RMPs) in feed forward mode [2]. Divertor detachment is feedback controlled on the target temperature using nitrogen injection in the divertor.

Pellets with ELM mitigation by RMPs

In a previous paper [3] it was shown that pellets can refuel the RMP pump-out using the application of pellet trains with a gradually increasing rate. Figure 1 shows the plasma with pellets applied promptly after activation of the RMP fields. In the scan, not shown here, the delay of the pellet train relative to the application of RMP fields was varied up to the point where the pellets start at the same time as the RMP fields. During the scan the overall duration of the density transient is about three energy confinement times (for more details see [4]). Such a duration of the refuelling transient is expected from a conventional ratio between particle and heat diffusivities. This indicates that the reduction of inward particle diffusion as predicted by gyro-kinetic theory [5] for hollow density profiles by pellets (figure 1i) is not significant in our case. In figure 1 the required pellet particle throughput to restore pre-RMP density during the stationary phase is about $\Phi_{pel}\sim5.6\times10^{21}$at/s (pellet size 1.4×1.4×1.5mm, pellet rate $f_{pel}=47Hz$) which is comparable to the RMP pump out rate $\Phi_{RMP}\sim1.7\times10^{21}$at/s as determined from

the time derivative of the plasma density after the RMP is switched on. In this context it is instructive to compare the time-averaged pellet fuelling rate with a normalised heating power: $\Phi_{pel}T_{i,\mathrm{ped}} / P_{aux} \sim 0.073$ where $T_{i,\mathrm{ped}} \sim T_{i,92} = 700eV$, $P_{aux} = 8.6MW$. This value is similar to that in our previous work $\Phi_{pel}T_{i,\mathrm{ped}} / P_{aux} \sim 0.05$ [3] despite the pellet fuelling rate and the pedestal temperature being different. Application of RMPs reduces both the pedestal density and the pedestal temperatures (mainly the ions) and consequently the pedestal pressure (see figure 1e). During the pellet refuelling phase the change of pedestal temperature is modest (compared to pump-out phase) and the ion pedestal pressure is even increased (fig. 2b in [4]). An unwanted side effect of pellet refuelling is the transition from ELM suppression to an ELMy regime, triggered by the first pellet (see figures 1g, 1h). A favourable observation, however, is that ELMs with pellet fuelling are not modulated by pellets and are still smaller than those without RMPs. This can be seen from the dimensionless quantity $(f_{ELM}\tau_E)^{-1}$ which is a proportional to the relative energy loss per ELM $\delta W_{ELM}/W$ assuming that

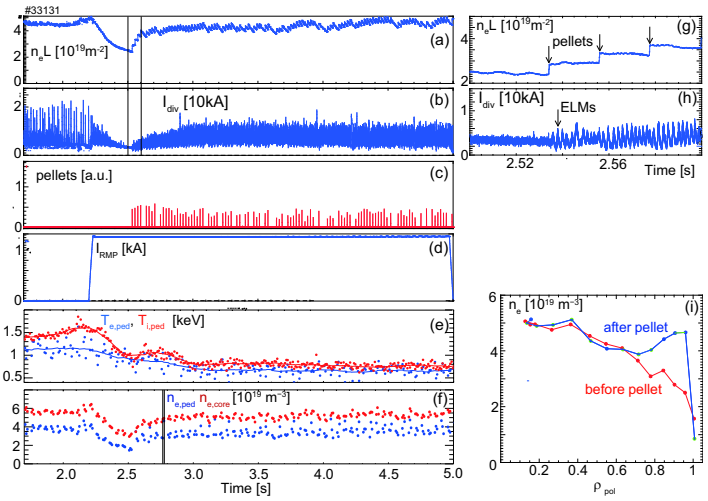

Figure 1. Temporal evolution of plasma parameters with ELM mitigation and pellet fuelling. (a) Line integrated density on the central chord, (b) outer divertor tile current, (c) pellet ablation radiation monitor, (d) RMP current, (e) electron and ion pedestal temperatures at $\rho_{pol} = \sqrt{\psi_N} \approx 0.92$ where ψ_N is the normalised poloidal magnetic flux (solid lines are the time-averaged values), (f) pedestal density and core density at $\rho_{pol} = 0.15$. (g) and (h) temporal details of the line integrated density and the divertor strike point current during the time interval shown by vertical lines in panels (a) and (b). (i) density profiles just before and after the pellet at the interval shown by vertical lines in panel (f).

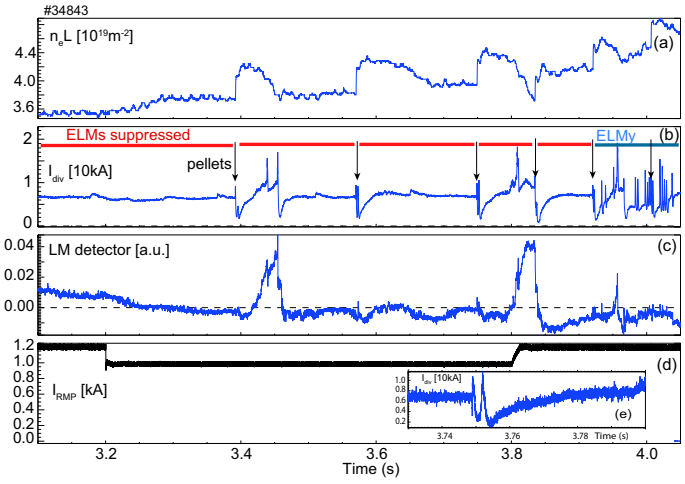

Figure 2. Temporal evolution of plasma parameters with ELM suppression and pellet fuelling at elevated triangularity. (a) line integrated density on central chord, (b) divertor strike point current, ELM suppressed and ELMy phases are indicated by red and blue bars, pellets timings by arrows; (c) locked mode detector signal, (d) RMP current, (e) insert, expansion of divertor strike point current around 3rd pellet at 3.7s.

ELM power loss is a constant fraction of the total power. Here f_{ELM} is the ELM frequency and τ_E is the thermal energy confinement time. During the pre RMP phase at $t = 2.15s$ this quantity is $(f_{ELM}\tau_E)^{-1} = (100Hz \times 0.066s)^{-1} = 15\%$ whereas during the pellet refuelling phase at $t = 3.0s$ it is $(f_{ELM}\tau_E)^{-1} = (450Hz \times 0.037s)^{-1} = 6\%$ i.e. about 3x smaller.

In order to maintain the ELM suppression phase the upper triangularity of the plasma should be elevated from $\delta_{up} = 0.1$ (as in figure 1) to $\delta_{up} = 0.28$ [2]. Figure 2 shows such a plasma fuelled by pellets of the same size as in figure 1 but with a lower rate. Similarly as in the low triangularity case the density increase by pellets causes the transition from the ELM suppression to the ELMy regime. The difference is that in the low triangularity case the first pellet already triggers an ELMy phase whereas at the elevated triangularity the ELM suppression phases are preserved in-between initial pellets (see fig. 2). Closer inspection shows that individual pellets trigger a prompt ELM during the ablation phase followed by a second ELM about 2.5ms later (fig. 2e). While the prompt ELM is typically associated with the high pressure plasmoid created by the pellet the nature of the second ELM is not clear. One possibility could be that pellets temporarily restore the pre-RMP density pedestal or that pellets induce departure from a narrow window of edge safety factor required for ELM suppression [2, 4].

Pellets with semi-detached plasmas

Figure 3 shows the traces of a plasma in which the density is simultaneously controlled by pellets and divertor detachment by nitrogen gas [6, 7]. Both quantities are controlled in feedback mode using bremsstrahlung emission as a proxy for the density and the divertor temperature deduced from divertor tile current. In the flat top phase the particle throughput due to pellets is $\Phi_{pel} \sim 18 \times 10^{21}$ at/s or normalised to the heat flux: $\Phi_{pel} T_{ped} / P_{aux} \sim 0.1$ (here the pellet size is 1.9×1.9×2mm, $f_{pel} \sim 60Hz$, $T_{ped} \sim 500eV$, $P_{aux} = 14MW$). This value of normalised pellet throughput is close to that found with RMPs.

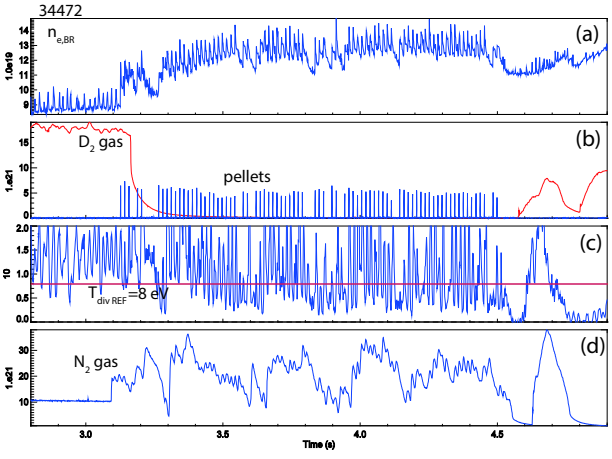

Figure 3. Temporal evolution of plasma parameters with semi-detached plasma and pellet fuelling. (a) line integrated density deduced from bremsstrahlung emission, (b) deuterium gas puff rate and pellet ablation light, (c) plasma temperature at the divertor outer strike point deduced from the tile current and its reference value for the feedback system (in red), (d) nitrogen gas puff rate.

Fig. 4 shows a side effect of the pellet

fuelling of semi-detached plasma: during the pellet train the divertor temperature oscillates by a factor of two (panel 4a). These perturbations propagate also to the nitrogen gas valve signal. The ELM signal in fig. 4c shows that the introduction of pellets changes the ELM character from regular to irregular bursts. This is reflected on the target probe signals where the temperature decreases during the transient ELM free phases and increases during the ELM bursts. This indicates that the modulation of divertor temperature is likely influenced by the modulation of the ELM frequency by pellets and not caused solely by a direct pellet cooling as one might expect. This means that the next step in development of this regime is the ELM mitigation under condition of pellet fuelling.

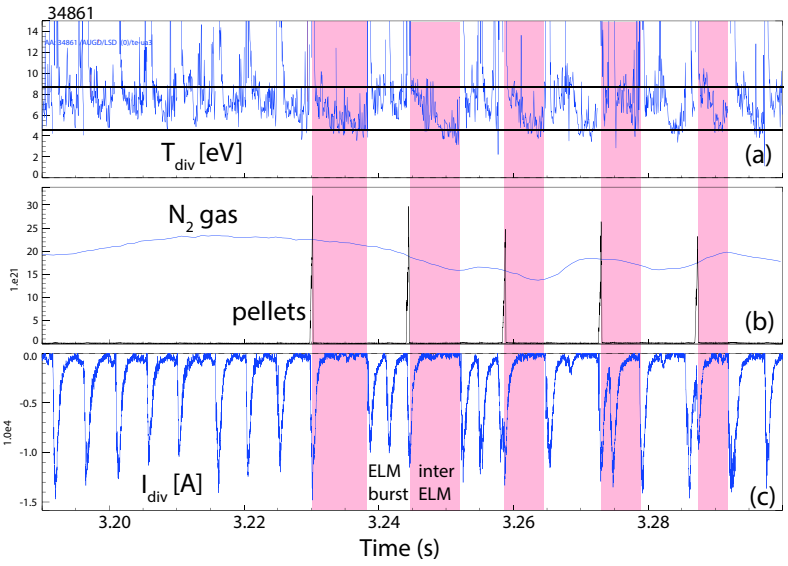

Figure 4. Detail of temporal evolution of plasma parameters with semi-detached plasma and pellet fuelling. (a) plasma temperature from divertor triple probe at divertor outer strike point, (b) nitrogen gas puff rate and pellet ablation light, (c) divertor tile current as ELM detector.

Conclusion

The paper examines the interaction between density control by pellets on the one side and the ELM control by RMPs or detachment control on the other side. Pellets generally cause the transition from ELM suppression to ELMy regime although ELMs remain mitigated (low δ) or less frequent (elevated δ) compared to pre RMP phase. Regarding the detachment the pellets modulate the divertor temperature, likely via ELMs and not by direct cooling. In both plasma regimes the normalised pellet particle throughput is similar, $\Phi_{pel} T_{\mathrm{ped}} / P_{aux} \sim 0.07\text{-}0.1$. Results underline the importance of pellet-ELM coupling in future control loop developments.

This work has been carried out within the framework of the EUROfusion Consortium and has received funding from the Euratom research and training programme 2014-2018 under grant agreement No 633053 and from the RCUK Energy Programme [grant number EP/P012450/1]. To obtain further information on the data and models underlying this paper please contact PublicationsManager@ukaea.ac.uk. The views and opinions expressed herein do not necessarily reflect those of the European Commission. Dr C M Roach is gratefully acknowledged for his valuable comments.

[1] Lang P T *et al* 2012 Nucl. Fusion **52** 024002
[2] Suttrop W *et al* 2017 Plasma Phys. Control. Fusion **59** 014050
[3] Valovič M *et al* 2016 Nucl. Fusion **56** 066009
[4] Valovič M *et al* 2018 Plasma Phys. Control. Fusion accepted
[5] Garzotti L *et al* 2014 Plasma Phys. Control. Fusion **56** 035004; Angioni C *et al* 2017 Nucl. Fusion **57** 116053
[6] Bernert M *et al* 2015 Plasma Phys. Control. Fusion **57** 014038
[7] Kallenbach A *et al* 2018 Plasma Phys. Control. Fusion **60** 045006